

Doc-Start

Structural bioinformatics

Sequence-structure relations of biopolymers

Christopher Barrett¹, Fenix W. Huang¹ and Christian M. Reidys^{1*}¹Virginia Bioinformatics Institute, 1015 Life Sciences Circle, Blacksburg, VA, USA

*To whom correspondence should be addressed.

Associate Editor: XXXXXXXX

Received on XXXXX; revised on XXXXX; accepted on XXXXX

Abstract

Motivation: DNA data is transcribed into single-stranded RNA, which folds into specific molecular structures. In this paper we pose the question to what extent sequence- and structure-information correlate. We view this correlation as structural semantics of sequence data that allows for a different interpretation than conventional sequence alignment. Structural semantics could enable us to identify more general embedded "patterns" in DNA and RNA sequences.

Results: We compute the partition function of sequences with respect to a fixed structure and connect this computation to the mutual information of a sequence-structure pair for RNA secondary structures. We present a Boltzmann sampler and obtain the *a priori* probability of specific sequence patterns. We present a detailed analysis for the three PDB-structures, 2JXV (hairpin), 2N3R (3-branch multi-loop) and 1EHZ (tRNA). We localize specific sequence patterns, contrast the energy spectrum of the Boltzmann sampled sequences versus those sequences that refold into the same structure and derive a criterion to identify native structures. We illustrate that there are multiple sequences in the partition function of a fixed structure, each having nearly the same mutual information, that are nevertheless poorly aligned. This indicates the possibility of the existence of relevant patterns embedded in the sequences that are not discoverable using alignments.

Availability: The source code is freely available at <http://staff.vbi.vt.edu/fenixh/Sampler.zip>

Contact: duckcr@vbi.vt.edu

Supplementary information: Supplementary material containing additional data tables are available at *Bioinformatics* online.

1 Introduction

2015 is the 25th year of the human genome project. A recent signature publication (The 1000 Genomes Project Consortium, 2015) is a comprehensive sequence alignment-based analysis of whole genome nucleotide sequence variation across global human populations. Notwithstanding the importance of this achievement, there is the possibility of information encoded as patterns in the genome that current methods cannot discover.

In this paper we study the information transfer from RNA sequences to RNA structures. This question is central to the processing of DNA data, specifically the role of DNA nucleotide sequences being transcribed into RNA, stabilized by molecular folding. In a plethora of interactions it is this specific configuration and not the particular sequence of nucleotides (aside from, say small docking areas, where specific bindings occur) that determines biological functionality. We find that here are multiple

sequences in the partition function of a fixed structure, each having nearly the same mutual information with respect to the latter, that are nevertheless poorly aligned. This indicates the possibility of the existence of relevant patterns embedded in the sequences that are not discoverable using alignments.

RNA, unlike DNA, is almost always single-stranded¹ and all RNA is folded. Here we only consider single-stranded RNA. An RNA strand has a backbone made of alternating sugar (ribose) and phosphate groups. Attached to each sugar is one of four bases—adenine (A), uracil (U), cytosine (C), or guanine (G). There are various types of RNA: messenger RNA (mRNA), ribosomal RNA (rRNA), transfer RNA (tRNA) and many others. Recent transcriptomic and bioinformatic studies suggest the existence of numerous of so called non-coding RNA, ncRNAs, that is RNA that does not translate into protein (Eddy, 2001; Cheng *et al.*, 2005).

¹ There are double-stranded RNA viruses

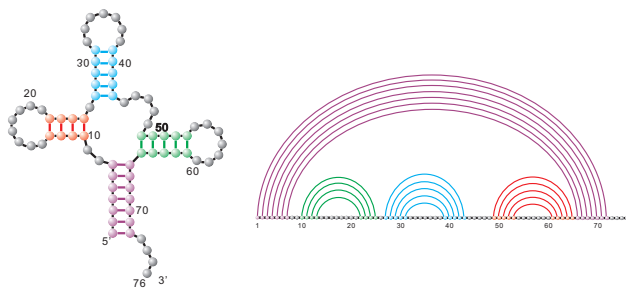


Fig. 1. tRNA: its secondary structure and its diagram presentation.

RNA realizes folded molecular conformations consistent with the Watson-Crick base as well as the wobble base pairs. In the following we consider RNA secondary structures, presented as diagrams obtained by drawing the sequence in a straight line and placing all Watson-Crick and Wobble base pairs as arcs in the upper half-plane, without any crossing arcs, see Fig. 1.

DNA information processing refers to replication, transcription and translation. Additionally, RNA information processing includes replication (Koonin *et al.*, 1989), reverse transcription (from RNA to DNA in e.g. retroviruses) (Temin and Mizutani, 1970) and a direct translation from DNA to protein² (McCarthy and Holland, 1965; Uzawa *et al.*, 2002).

In the following we offer an alternative view of DNA-RNA information processing. We focus on the information transfer from DNA/RNA sequences to the folded RNA (after transcription). We speculate that the sequential DNA information may transcribe into single-stranded RNA in order to allow subsequent biological processes to interpret DNA data.

DNA data are viewed as sequences of nucleotides. We currently use sequence alignment tools as a means of arranging the sequences of DNA, RNA, or proteins to identify regions of similarity that may be a consequence of functional, structural, or evolutionary relationships between the sequences (Mount, 2004). Here we suggest that the transcription into RNA with the implied self-folding is a way of lifting DNA information to a new and different level: RNA structures provide sequence semantics.

In order to study this idea we consider the folding of RNA sequences into minimum free energy (mfe) secondary structures (Waterman, 1978). Pioneered by Waterman more than three decades ago (Smith and Waterman, 1978) and subsequently studied by Schuster *et al.* (Schuster *et al.*, 1994) in the context of the RNA toy world (Schuster, 1997) there is detailed information about this folding. In particular we have fairly accurate energy values for computing loop-based mfe (Mathews *et al.*, 1999, 2004; Turner and Mathews, 2010) that are employed by the folding algorithms (Zuker and Stiegler, 1981; Hofacker *et al.*, 1994). More work has been done on loop-energy models in (Mathews, 2004; Do *et al.*, 2006). We plan on a more detailed analysis of the framework proposed here in the context of the MC-model (Parisien and Major, 2008).

In (McCaskill, 1990) McCaskill observed that the dynamic programming routines folding mfe structures (McCaskill, 1990) allows one to compute the partition function of all possible structures for a given sequence. The partition function is tantamount to computing the probability space of structures that a fixed sequence is compatible with. Predictions such as base pairing probabilities are obtained in (Hofacker *et al.*, 1994; Hofacker, 2003) and are parallelized in (Fekete *et al.*, 2000). (Tacker *et al.*, 1996; Ding and Lawrence, 2003) derives a statistically valid sampling of secondary structures in the

Boltzmann ensemble and calculates the sampling statistics of structural features.

In view of the above we are led to consider the “dual” of McCaskill’s partition function, i.e. the partition function of all sequences that are compatible with a fixed structure. More generally we consider the pairing

$$\varepsilon: \mathcal{Q}_4^n \times \mathcal{S}_n \longrightarrow \mathbb{R}^+, \quad (1)$$

where \mathcal{Q}_4^n and \mathcal{S}_n denote the space of sequences, σ , and the space of secondary structures, S , respectively and $\varepsilon(\sigma, S) = e^{-\frac{\eta(\sigma, S)}{RT}}$ as well as the energy function $\eta(\sigma, S) \in \mathbb{R}$ are discussed in Section 2.1.

We show in Section 3 how ε allows us to capture the mutual information between sequences and structures, where the mutual information between x and y is given by

$$I(x, y) = \mathbb{P}(x, y) \log \left(\frac{\mathbb{P}(x, y)}{\mathbb{P}(x)\mathbb{P}(y)} \right).$$

Here $\mathbb{P}(x, y)$ denotes the joint probability distribution. **In our case,** $\mathbb{P}(\sigma, S) = \varepsilon(\sigma, S) / \sum_{\sigma \in \mathcal{Q}_4^n, S \in \mathcal{S}_n} \varepsilon(\sigma, S)$, $\mathbb{P}(\sigma) = \sum_{S \in \mathcal{S}_n} \mathbb{P}(\sigma, S)$, and $\mathbb{P}(S) = \sum_{\sigma \in \mathcal{Q}_4^n} \mathbb{P}(\sigma, S)$.

In addition, ε allows us to express folding by considering

$$\{S \mid \varepsilon(\sigma, S) = \max_{S \in \mathcal{S}_n} \varepsilon(\sigma, S)\},$$

and inverse folding as to compute $\{\sigma \mid \varepsilon(\sigma, S) = \max_{\sigma \in \mathcal{Q}_4^n} \varepsilon(\sigma, S)\}$, for fixed S . Accordingly, the dual to folding is tantamount to computing for fixed S

$$\{\sigma \mid \varepsilon(\sigma, S) = \max_{\sigma \in \mathcal{Q}_4^n} \varepsilon(\sigma, S)\}.$$

This has direct implications to the “inverse” folding of structures. Inverse folding is by construction about the sequence constraints induced by a fixed structure while avoiding competing configurations. Point in case: it has been observed in (Busch and Backofen, 2006) that starting with a sequence that is mfe w.r.t. to a fixed structure, without necessarily folding into it, constitutes a significantly better initialization than starting with a random sequence.

The paper is organized as follows: we first recall in Section 2.1 **the decomposition of secondary structures as well as the loop-based thermodynamic model**. This in turn facilitates (Sections 2.3 and 2.4) the derivation of the partition function and Boltzmann sampling. In Sections 2.3 and 2.4 we compute $Q(S)$, Boltzmann sampling and the *a priori* probability of sequence patterns.

2 Method

2.1 Secondary structures and loop decomposition

RNA structures can be represented as diagrams where we consider the labels of the sequence to be placed on the x -axis and the Watson-Crick as well as Wobble base pairs drawn as arcs in the upper half plane see Fig. 1. That is, we have a vertex-labeled graph whose vertices are drawn on a horizontal line labeled by $[n] = \{1, 2, \dots, n\}$, presenting the nucleotides of the RNA sequence and the linear order of the vertices from left to right indicates the direction of the backbone from 5'-end to 3'-end. Furthermore each vertex can be paired with at most one other vertex by an arc drawn in the upper half-plane. Such an arc, (i, j) , represents the base pair between the i th and j th nucleotide³. **Two arcs (i, j) and (r, s) are called crossing if and only if $i < r$ and $i < r < j < s$ holds. An RNA structure is called**

² in cell-free systems, using extracts from *E. coli* that contains ribosomes

³ here we assume $j - i > 3$ to meet the minimum size requirement of a hairpin loop.

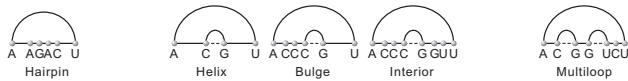


Fig. 2. Hairpin-, helix-, bulge-, interior- and multi-loops in secondary structures.

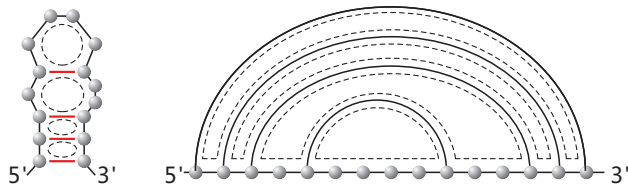


Fig. 3. Loops and their correspondence in a diagram.

pseudoknot-free, or secondary structure, if it does not contain any crossing arcs. Furthermore, the arcs of a secondary structure can be endowed with the partial order: $(r, s) \prec (i, j)$ if and only if $i < r < s < j$.

A filtration based on the individual contributions of base pairs of RNA structures was computed via the Nussinov model (Nussinov *et al.*, 1978). (Smith and Waterman, 1978) were the first bringing energy into the picture, computing the free-energy accurately via loops. A loop in a diagram consists of a sequence of intervals on the backbone $([a_i, b_i])_i$, $1 \leq i \leq k$, where (a_1, b_k) , (b_i, a_{i+1}) , for all $1 \leq i < k$ are base pairs. By construction, each base pair (i, j) is involved in exactly two loops: one where (i, j) is maximal respect to \prec , and one where (i, j) is not. Furthermore, there is a distinguished loop, L_{ex} , called the exterior loop, where $a_1 = 1$, $b_k = n$ and (a_1, b_k) is not a base pair. Depending on the number of base pairs, and unpaired bases inside a loop, a loop is categorized as hairpin-, containing exactly one base pair and one interval, helix-, containing two base pairs and two empty intervals, interior-, containing two non-empty intervals and two base pairs, bulge-, containing two base pairs and two intervals, where one of them is empty and the other one is not and multi-loops, see Fig. 2 and Fig. 3.

Further developments on RNA secondary structure prediction were given by (Zuker and Stiegler, 1981; Hofacker *et al.*, 1994). In particular, accurate thermodynamic energy parameters can be found in (Mathews *et al.*, 1999, 2004; Turner and Mathews, 2010; Parisien and Major, 2008; Deigan *et al.*, 2009; Hajdin *et al.*, 2013; Lorenz *et al.*, 2016).

In the following, we briefly recall the Turner energy model (Mathews *et al.*, 1999, 2004; Turner and Mathews, 2010) for RNA secondary structures. Let $\sigma = (\sigma_1, \sigma_2, \dots, \sigma_n)$ be a sequence, where $\sigma_i \in \{A, U, C, G\}$ for all $1 \leq i \leq n$. To an arbitrary loop, L , we assign the energy $\eta(\sigma, L)$, where $\eta(\sigma, L_{ex}) = 0$ and $\eta(\sigma, L)$ depends on two factors: its type and the underlying backbone. Specifically this is the number of bases pairs, the number of unpaired bases and the particular nucleotides involved. The energy of a structure S over an RNA sequence σ is then given by the sum of the energies of individual loops i.e.,

$$\eta(\sigma, S) = \sum_{L \in S} \eta(\sigma, L). \quad (2)$$

A hairpin, L_H is a loop having exactly one base pair with a non-empty interval containing k unpaired bases, where $k \geq 3$ due to flexibility constraints imposed by the backbone of the molecule.

In case of $3 \leq k \leq 4$ we call L a tetra-loop, which has a particular energy that depends on the two nucleotides incident to its unique arc $(\sigma_i, \sigma_{i+k+1})$ as well as the particular nucleotides corresponding to the unpaired bases of its unique non-empty interval $(\sigma_{i+1}, \dots, \sigma_{i+k})$.

For any other number of unpaired bases, k , the energy calculation depends only on k and not the particular nucleotide sequence, except of $(\sigma_i, \sigma_{i+k+1})$ and σ_{i+1} and σ_{i+k} . We have

$$\eta(\sigma, L_H) = \begin{cases} \eta_H((\sigma_i, \sigma_{i+k+1}), \sigma_{i+1}, \dots, \sigma_{i+k}) & \text{if } 3 \leq k \leq 4 \\ \eta_H((\sigma_i, \sigma_{i+k+1}), \sigma_{i+1}, \sigma_{i+k}, k) & \text{otherwise.} \end{cases} \quad (3)$$

An interior, bulge or helix loop, L_* , can be represented as two intervals and two base pairs $L_* = \{[i, r], [s, j], (i, j), (r, s)\}$. The energy of L_* is computed as

$$\eta(\sigma, L_*) = \begin{cases} \eta_*(\sigma_i, \sigma_j, (\sigma_r, \sigma_s)) & \text{(helix)} \\ \eta_*(\sigma_i, \sigma_j, (\sigma_r, \sigma_s), \sigma_{i+1}, \sigma_{r-1}, \sigma_{s+1}, \sigma_{j-1}, k_1) & \text{(bulge)} \\ \eta_*(\sigma_i, \sigma_j, (\sigma_r, \sigma_s), \sigma_{i+1}, \sigma_{r-1}, \sigma_{s+1}, \sigma_{j-1}, k_1, k_2) & \text{(interior)} \end{cases} \quad (4)$$

where $k_1 = \max\{r-i-1, j-s-1\}$ and $k_2 = \min\{r-i-1, j-s-1\}$.

A multi-loop L_M contains p base pairs and p intervals, some of which being possibly empty, where $p \geq 3$. $\eta_M(\sigma, L_M)$ is computed by

$$\eta_M(\sigma, L_M) = \alpha + p \cdot \beta + u \cdot \gamma. \quad (5)$$

Here α is the constant multi-loop penalty, β and γ are constants and u is the number of all unpaired bases contained in the respective intervals.

2.2 The partition function

Definition 1. Let S be a secondary structure over n nucleotides. Then the partition function of S is given by

$$Q(S) = \sum_{\sigma \in \mathcal{Q}_4^n} e^{-\frac{\eta(\sigma, S)}{RT}}, \quad (6)$$

where $\eta(\sigma, S)$ is the energy of S on σ , R is the universal gas constant and T is the temperature.

In analogy to the partition function of a fixed sequence $Q(\sigma)$ (McCaskill, 1990), $Q(S)$ can be computed recursively. Given the structure S , we consider an arbitrary arc (i, j) , where $i < j$. Let $S_{i,j}$ denote the substructure of S over the interval $[i, j]$. Since S contains no crossing arcs all arcs of $S_{i,j}$ are contained in $[i, j]$, whence $S_{i,j}$ is well defined. Let

$$Q(\sigma_i, \sigma_j) = \sum_{\substack{\sigma \in \mathcal{Q}_4^{j-i+1} \\ \sigma|_{[i, j]} = \sigma|_{[i, j]}}} e^{-\frac{\eta(\sigma, S_{i,j})}{RT}}.$$

Since S has no crossing arcs, the interval $[i, j]$ is covered by the arc (i, j) , i.e. (i, j) induces a loop L for which (i, j) is maximal. Suppose L consist of intervals $[i, p_1], [q_1, p_2], \dots, [q_k, j]$, where $(p_1, q_1) \dots, (p_k, q_k)$ are L -arcs different from (i, j) . Removal of L renders substructures covered by $(p_1, q_1) \dots, (p_k, q_k)$. Considering all combinations of the nucleotides in position p_i and q_i , $1 \leq i \leq k$, we derive the following recursion, see Fig. 4:

$$Q(\sigma_i, \sigma_j) = \sum_{\sigma_{p_t}, \sigma_{q_t} \in \mathcal{Q}_4^n} e^{-\frac{\eta(\sigma, L)}{RT}} \prod_t^k Q(\sigma_{p_t}, \sigma_{q_t}). \quad (7)$$

The partition function $Q(S)$ is then obtained as the weighted sum of the terms $Q(\sigma_{a_t}, \sigma_{b_t})$, where (a_t, b_t) , $\forall 1 \leq t \leq k$ are base pairs in the exterior loop L_{ex} :

$$Q(S) = \sum_{\sigma_{a_t}, \sigma_{b_t} \in \mathcal{Q}_4^n} e^{-\frac{\eta(\sigma, L_{ex})}{RT}} \prod_t^k Q(\sigma_{a_t}, \sigma_{b_t}). \quad (8)$$

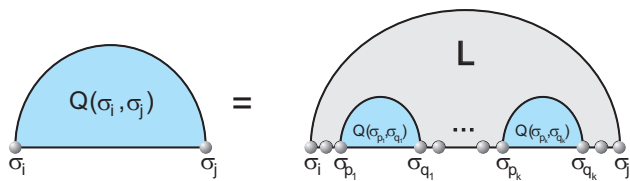


Fig. 4. The recursion for computing the partition function $Q_T(\sigma_i, \sigma_j)$.

Remark. The routine of computing $Q(S)$ is similar to the one for finding an optimal sequence for a given structure in (Busch and Backofen, 2006). Passing to a topological model for RNA structures (Orland and Zee, 2002; Penner, 2004; Bon et al., 2008; Reidys et al., 2011), the above recursions can be extended to pseudoknotted RNA structures, i.e. RNA structures containing crossing arcs. The key here is a general bijection between maximal arcs and topological boundary components (loops).

2.3 Boltzmann sampling and patterns

Having computed the partition function $Q(S)$ as well as the $Q(\sigma_i, \sigma_j)$ terms, puts us in position to Boltzmann sample sequences for fixed secondary structure S . Here the probability of a sequence σ to be sampled is given by

$$\mathbb{P}(\sigma|S) = \frac{e^{-\frac{\eta(\sigma, S)}{RT}}}{Q(S)}.$$

We build σ recursively from top to bottom, starting with the exterior loop, L_{ex} . Suppose (p_t, q_t) are base pairs contained in L_{ex} and let u denote the number of unpaired bases in L_{ex} . Since $\eta(\sigma, L_{ex}) = 0$, the unpaired nucleotides in L_{ex} are sampled uniformly, i.e., with probability $1/4$. Then the probability of the event σ_r being the nucleotide in position $r \in L_{ex}$, is given by

$$\mathbb{P}(\sigma_r|S) = \frac{e^{-\frac{\eta(\sigma, L_{ex})}{RT}} \prod_{t=1}^k Q(\sigma_{p_t}, \sigma_{q_t})}{Q(S)} = \frac{(\frac{1}{4})^u \prod_{t=1}^k Q(\sigma_{p_t}, \sigma_{q_t})}{Q(S)},$$

where the dependence on σ_r of the RHS stems from $\sigma|_r = \sigma_r$ or potentially $p_t = r$ or $q_t = r$. We continue the process inductively from top to bottom. Suppose we are given a loop L with the maximal base pair (i, j) . Since any two arcs in S are not crossing, any arc (i, j) is contained in exactly two loops (except for the exterior loop) where (i, j) is the maximal arc for one and not for the other. As a result, the nucleotides σ_i, σ_j associated with (i, j) are sampled as part of the preceding loop⁴. It remains to sample the nucleotides other than σ_i and σ_j in L . Let σ_r be the nucleotides in L and $r \neq i, j$. The probability of the event σ_r being the nucleotide in position $r, r \neq i, j$ is given by

$$\mathbb{P}(\sigma_r|S) = \frac{e^{-\frac{\eta(\sigma, L)}{RT}} \prod_{t=1}^k Q(\sigma_{p_t}, \sigma_{q_t})}{Q(\sigma_i, \sigma_j)}.$$

Here (p_t, q_t) , for $1 \leq t \leq k, k \geq 0$ are base pairs contained in L , that are different from (i, j) . In particular, L is a hairpin loop in case of $k = 0$, an interior-, bulge- or a helix-loop in case of $k = 1$, and a multi-loop for $k \geq 2$.

By construction, for any arc there is a unique loop for which the arc is maximal and a unique loop where the arc is not. As a result, the probability

⁴ in which (i, j) is not maximal

of a sequence σ to be sampled is given by

$$\mathbb{P}(\sigma|S) = \prod_{(i,j) \in S} \frac{e^{-\frac{\eta(\sigma, L(i,j))}{RT}} \prod_{t=1}^k Q(\sigma_{p_t}, \sigma_{q_t})}{Q(\sigma_i, \sigma_j)} \cdot \frac{(\frac{1}{4})^u \prod_{t=1}^k Q(\sigma_{p_t}, \sigma_{q_t})}{Q(S)}$$

In view of eq. (2) and the fact that the term $Q(\sigma_{p_t}, \sigma_{q_t})$ appears exactly once for each arc (p_t, q_t) , we arrive at

$$\prod_{(i,j) \in S} \left(\prod_{t=1}^k Q(\sigma_{p_t}, \sigma_{q_t}) \right) = \prod_{(i,j) \in S} Q(\sigma_i, \sigma_j).$$

This in turn implies

$$\mathbb{P}(\sigma|S) = \frac{\left(\prod_{(i,j) \in S} e^{-\frac{\eta(\sigma, L(i,j))}{RT}} \right) \left(\prod_{(i,j) \in S} Q(\sigma_i, \sigma_j) \right)}{Q(S) \prod_{(i,j) \in S} Q(\sigma_i, \sigma_j)} = \frac{e^{-\frac{\eta(\sigma, S)}{RT}}}{Q(S)}.$$

The time complexity for computing the partition function of a structure and Boltzmann sampling depends solely on the complexity of the energy function, $\eta(\sigma, L)$. Clearly, there are $O(n)$ loops in the structure and reviewing eq. (3), eq. (4) and eq. (5), at most eight nucleotides are taken into account. From this we can conclude that the time complexity is $O(n)$, as claimed.

Next, we compute the probability of a given sequence pattern, i.e. the subsequence of σ over $[i, j]$ being $p_{i,j}$. We shall refer to a sequence containing $p_{i,j}$ by $\sigma|_{p_{i,j}}$.

The partition function of all sequences σ containing $p_{i,j}$ is given by

$$Q(S|p_{i,j}) = \sum_{\sigma|_{p_{i,j}} \in \mathcal{Q}_4^n} e^{-\frac{\eta(\sigma, S)}{RT}} \quad (9)$$

and the probability of $p_{i,j}$ is $\mathbb{P}(p_{i,j}|S) = \frac{Q(S|p_{i,j})}{Q(S)}$.

We have shown how to compute $Q(S)$ recursively in Section 2.3. It remains to show how to compute $Q(S|p_{i,j})$. To do this we use the same routine as for computing $Q(S)$, but eliminating any subsequences that are not compatible with $p_{i,j}$. By construction, for any pattern, this process has the same time complexity as computing $Q(S)$.

3 Discussion

Let us begin by discussing the mutual information of sequence-structure pairs. Then we ask to what extent does a structure determine particular sequence patterns and finally derive a criterion that differentiates native from random structures.

The mutual information of a sequence-structure pair can be computed by normalizing ϵ

$$\mathbb{P}(\sigma, S) = \frac{e^{-\frac{\eta(\sigma, S)}{RT}}}{\sum_{\sigma \in \mathcal{Q}_4^n} \sum_{S \in \mathcal{S}_n} e^{-\frac{\eta(\sigma, S)}{RT}}},$$

where $U = \sum_{\sigma \in \mathcal{Q}_4^n} \sum_{S \in \mathcal{S}_n} e^{-\frac{\eta(\sigma, S)}{RT}}$ is a constant. Then we have

$$I(\sigma, S) = \left(e^{-\frac{\eta(\sigma, S)}{RT}} \log \frac{e^{-\frac{\eta(\sigma, S)}{RT}}}{Q(\sigma)Q(S)} \right) / U + \left(e^{-\frac{\eta(\sigma, S)}{RT}} \log U \right) / U.$$

Since U is a large constant, we observe that one term of $\mathbb{P}(\sigma, S)$, namely

$$e^{-\frac{\eta(\sigma, S)}{RT}} \log \frac{e^{-\frac{\eta(\sigma, S)}{RT}}}{Q(S)Q(\sigma)}$$

contributes the most. Accordingly, $Q(S)$ and $Q(\sigma)$ allow us to quantify how a probability space of structures determines a probability space of sequences.

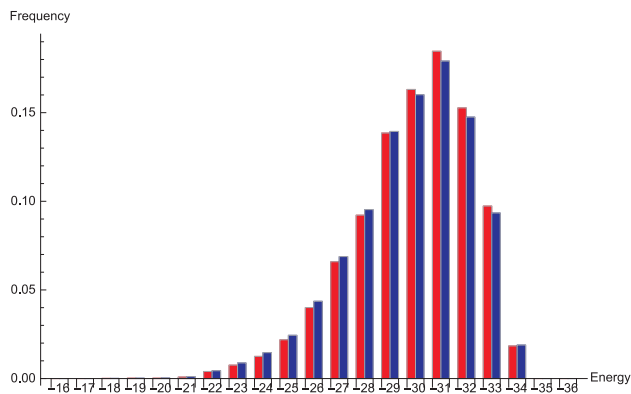


Fig. 8. The energy distribution of the Boltzmann sample for 2JXV. We display the frequency of sequences having a particular energy (blue) and the frequency of sequences that fold into 2JXV (red).

The energy distribution of the Boltzmann sample is given in Fig. 10 (A) and we display the $\Delta\eta(\sigma)$ -data in Fig. 10 (B) where we contrast the data with $\Delta\eta(\sigma)$ -values obtained from Boltzmann sampling 10^4 sequences of 5 random structures of the same length. We observe that the $\Delta\eta(\sigma)$ -values for 2N3R are distinctively lower than those for random structures.

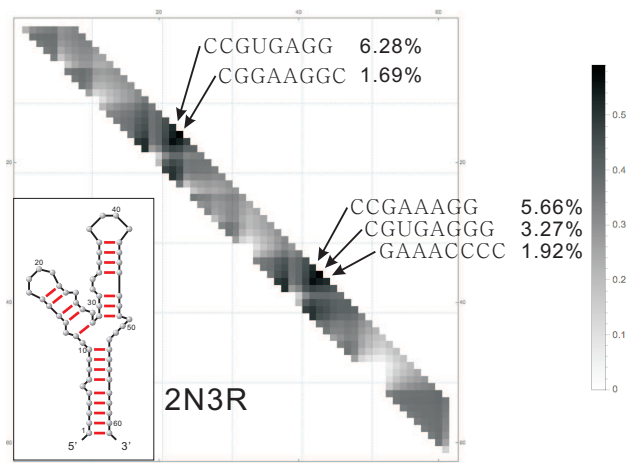


Fig. 9. The secondary structure of 2N3R and its heat-map. We show the most frequent patterns for the largest interval having $R_{i,j} > 0.52$. The sample size is 10^4 .

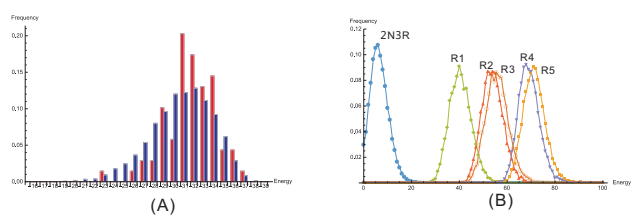


Fig. 10. (A) The energy distribution of Boltzmann sampled sequences. The frequency of sequences having a particular energy level (blue), the frequency of sequences folding into 2N3R (red). (B) $\Delta\eta(\sigma)$ -data of 2N3R versus $\Delta\eta(\sigma)$ -data of five random structures.

The PDB structure 1EHZ (Shi and Moore, 2000) is a tRNA over 76 nucleotides exhibiting a 4-branch multi-loop. We display the heat-map of 1EHZ in Fig. 11. The IFR is 1.3×10^{-3} w.r.t. our Boltzmann sample of size 10^4 and we display the energy distribution of the sampled sequences in Fig. 12 (A). Interestingly we still find many inverse fold solutions by just Boltzmann sampling $Q(S)$ and these sequences are not concentrated at low free energy values.

In Fig. 12 (B) we display the $\Delta\eta(\sigma)$ -data and contrast them with those obtained by the Boltzmann samples of five random structures. We observe a significant difference between the $\Delta\eta(\sigma)$ -distribution of the 1EHZ sample and those of the random structures.

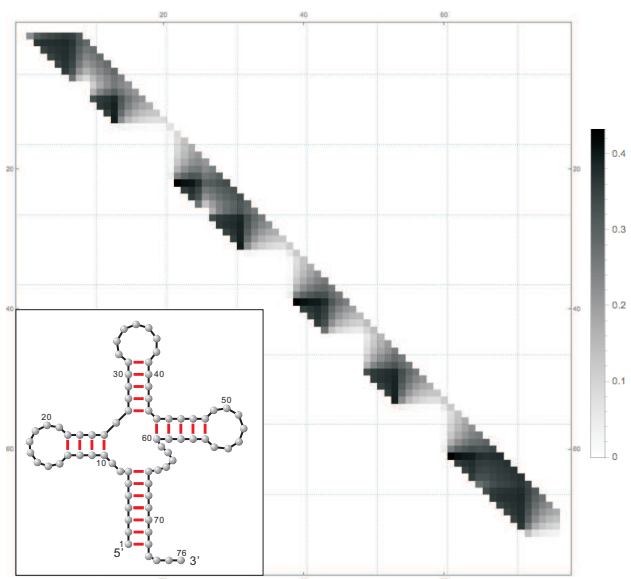


Fig. 11. The secondary structure of 1EHZ and its heat-map. We display the most frequent sampled pattern for the largest interval having $R_{i,j} > 0.52$. The sample size is 10^4 .

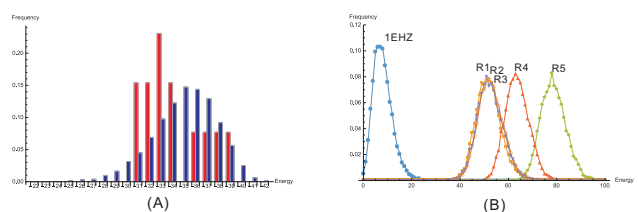


Fig. 12. (A) The energy distribution of the Boltzmann sampled sequences. The frequency of sequences having a particular energy level (blue), the frequency of sequences folding into 1EHZ (red). (B) $\Delta\eta(\sigma)$ -data of 1EHZ versus $\Delta\eta(\sigma)$ -data of five random structures.

The three above examples indicate that sequence-structure correlations can be used to locate regions where specific embedded patterns arise. Furthermore we observe that studying $Q(S)$ has direct implications for inverse folding. This is in agreement with the findings in (Busch and Backofen, 2006), but leads to deriving alternative, unbiased starting sequences for inverse folding. Although at present we can only estimate the mutual information, we can conclude that there are sequences that cannot be aligned but obtain almost identical mutual information.

We observe that biological relevant sequences exhibit a $\Delta\eta(\sigma)$ -signature distinctive different from that of random structures. Therefore, the $\Delta\eta(\sigma)$ -signature is capable of distinguishing biological relevant structures from random structures. In (Miklós *et al.*, 2005) the expected free energy and variance of the Boltzmann ensemble of a given sequence has been employed in order to distinguish biologically functional RNA sequences from random sequences. This result is in terms of the pairing $\varepsilon: \mathcal{Q}_4^n \times \mathcal{S}_n \rightarrow \mathbb{R}^+$, dual⁵ to our approach. Our $\Delta\eta(\sigma)$ -signature characterize the naturality of a fixed structure and (Miklós *et al.*, 2005) the naturality of a fixed sequence. Accordingly, $Q(S)$ augments the analysis of $Q(\sigma)$ in a natural way, capturing the correlation between RNA sequences and structures.

As a result, sequences carry embedded patterns that cannot be understood by considering the sequence of nucleotides. At this point we have no concept of what these patterns are and provided in Section 2.4 a rather conventional notion of “embedded pattern”. However, even when considering specific nucleotide patterns in hairpin loops, we observe significant context dependence on the structure. Other loops affect the energy of the hairpin loop and thus determine this particular subsequence. We observe that the embedded patterns can, for certain structures, be quite restricted, possibly elaborate and are not entirely obvious. In any case, the analysis cannot be reduced to conventional sequence alignment. The heat-maps introduced here identify the regions for which only a few select patterns appear and computed the *a priori* probabilities of their occurrence.

This type of analysis will be carried out for the far more advanced MC-model (Parisien and Major, 2008), incorporating non-canonical base pairs, SHAPE-directed model for long RNAs (Deigan *et al.*, 2009; Hajdin *et al.*, 2013). This will in particular enable us to have a closer look at the hairpins of the tRNA structure. In addition we believe that this line of work may enable us to arrive at non-heuristic inverse foldings.

Folding of RNA secondary structures including pseudoknots is studied in (Rivas and Eddy, 1999) by extending the dynamic programming paradigm introducing substructures with a gap. The framework generates a particular, somewhat subtle class of pseudoknot structures, discussed in detail in (Rivas and Eddy, 2000). A specific, multiple context-free grammar (MCFG) for pseudoknotted structures is designed (Rivas and Eddy, 1999), employing a vector of nonterminal symbols referencing a substructure with a gap.

Our results facilitate the Boltzmann sample RNA sequences for pseudoknotted structures. Let $S_{i,j;r,s}$ denote a substructure with a gap where (i, j) , (r, s) are base pairs and $Q(\sigma_i, \sigma_j; \sigma_r, \sigma_s)$ denote the partition function of $S_{i,j;r,s}$, then one can compute $Q(\sigma_i, \sigma_j)$ following the MCFG given by (Rivas and Eddy, 1999).

A different approach was presented in (Penner and Waterman, 1993; Penner, 2004), where topological RNA structures have been introduced (Penner and Waterman, 1993; Penner, 2004). In difference to (Rivas and Eddy, 1999), which was driven by the dynamic programming paradigm, topological structures stem from the intuitive idea to just “draw” their arcs on a more complex topological surface in order to resolve crossings. Random matrix theory (von Neumann and Goldstine, 1947) facilitates the classification and expansion of pseudoknotted structures in terms of topological genus (Orland and Zee, 2002; Bon *et al.*, 2008) and in (Reidys *et al.*, 2011) a polynomial time, loop-based folding algorithm of topological RNA structures was given. The results in this paper are for representation purposes formulated in terms of loops. However they were originally developed in the topological framework, in which loops become topological boundary components. This means that we can extend our framework to pseudoknot structures. The key then is of course to be able to recursively compute the novel partition function, i.e. an unambiguous

grammar. Recent results (Huang and Reidys, 2016) associate a topological RNA structure with a certain, arc-labeled secondary structure, called λ -structure. The resulting disentanglement gives rise to a context free grammar for RNA pseudoknot structures (Huang and Reidys, 2016)⁶. We illustrate this correspondence in Fig 13. This finding facilitates to extend all our results to pseudoknotted structures and offers insight in patterns and inverse folding of more general RNA structure classes as well as RNA-RNA interaction complexes.

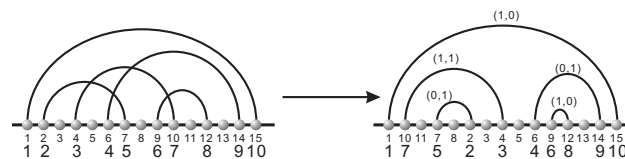


Fig. 13. Disentanglement: by means of permuting the backbone of a pseudoknotted structure one resolves all crossings.

As mentioned above, the present analysis is just a first step and discusses embedded patterns in the sense of subsequent nucleotides. However our framework can deal with any embedded pattern. We think a deeper, conceptual analysis has to be undertaken aiming at identifying how a collection of structures provides sequence semantics. Quite possibly this can be done in the context of formal languages. We speculate that advancing this may lead to a novel class of embedded pattern recognition algorithms beyond sequence alignment.

4 Acknowledgments

Special thanks to Michael Waterman and Peter Stadler for their input on this manuscript. We gratefully acknowledge the help of Kevin Shinpaugh and the computational support team at VBI, Rebecca Wattam, Henning Mortveit, Madhav Marathe and Reza Rezazadegan for discussions. Many thanks for the constructive feedback of the anonymous reviewers and their suggestions.

References

- Bon, M., Vernizzi, G., Orland, H., and Zee, A. (2008). Topological classification of RNA structures. *J. Mol. Biol.*, **379**, 900–911.
- Bonneau, E., Girard, N., Lemieux, S., and Legault, P. (2015). The NMR structure of the II-III-VI three-way junction from the neurospora VS ribozyme reveals a critical tertiary interaction and provides new insights into the global ribozyme structure. *RNA*, **21**, 1621–1632.
- Busch, A. and Backofen, R. (2006). INFO-RNA—a fast approach to inverse rna folding. *Bioinformatics*, **22**(15), 1823–31.
- Cevce, M., Thibaudeau, C., and Plavec, J. (2008). Solution structure of a let-7 miRNA:lin-41 mRNA complex from *C. elegans*. *Nucleic Acids Res.*, **36**, 2330–2337.
- Cheng, J., Kapranov, P., Drenkow, J., Dike, S., Brubaker, S., Patel, S., Long, J., Stern, D., Tammana, H., Helt, G., Sementchenko, V., Piccolboni, A., Bekiranov, S., Bailey, D. K., Ganesh, M., Ghosh, S., Bell, I., Gerhard, D. S., and Gingeras, T. R. (2005). Transcriptional maps of 10 human chromosomes at 5-nucleotide resolution. *Science*, **308**(5725), 1149–54.

⁵ the flip side of the coin, so to speak

⁶ More precisely, a λ -structures corresponds one-to-one to a pseudoknotted structure together with some additional information, i.e. a specific permutation of its backbone

- Deigan, K. E., Li, T. W., Mathews, D. H., and Weeks, K. M. (2009). Accurate SHAPE-directed RNA structure determination. *Proc. Natl. Acad. Sci. USA*, **106**(1), 87–102.
- Ding, Y. and Lawrence, C. E. (2003). A statistical sampling algorithm for RNA secondary structure prediction. *Nucleic Acids Res.*, **31**, 7280–7301.
- Do, C., Woods, D., and Batzoglou, S. (2006). Contrafold: RNA secondary structure prediction without physics-based models. *Bioinformatics*, **22**(14), e90–8.
- Eddy, S. R. (2001). Non-coding RNA genes and the modern rna world. *Nat. Rev. Genet.*, **2**(12), 919–29.
- Fekete, M., Hofacker, I., and Stadler, P. (2000). Prediction of RNA base pairing probabilities on massively parallel computers. *J. Comput. Biol.*, **7**, 171–182.
- Hajdin, C. E., Bellaousov, S., Huggins, W., Leonard, C. W., Mathews, D. H., and Weeks, K. M. (2013). Accurate SHAPE-directed RNA secondary structure modeling, including pseudoknots. *Proc. Natl. Acad. Sci. USA*, **110**(14), 5498–5503.
- Hofacker, I. L. (2003). The vienna RNA secondary structure server. *Nucl. Acids Res.*, **31**, 3429–3431.
- Hofacker, I. L., Fontana, W., Stadler, P. F., Bonhoeffer, L. S., Tacker, M., and Schuster, P. (1994). Fast folding and comparison of RNA secondary structures. *Monatsh. Chem.*, **125**, 167–188.
- Huang, F. and Reidys, C. M. (2016). Topological language for RNA. arXiv:1605.02628.
- Koonin, E. V., Gorbalenya, A. E., and Chumakov, K. M. (1989). Tentative identification of RNA-dependent RNA polymerases of dsRNA viruses and their relationship to positive strand RNA viral polymerases. *FEBS Lett.*, **252**(1-2), 42–6.
- Lorenz, R., Luntzer, D., Hofacker, I. L., Stadler, P. F., and Wolfinger, M. (2016). SHAPE directed RNA folding. *Bioinformatics*, **32**(1), 145–147.
- Mathews, D., Sabina, J., Zuker, M., and Turner, D. (1999). Expanded sequence dependence of thermodynamic parameters improves prediction of RNA secondary structure. *J. Mol. Biol.*, **288**, 911–940.
- Mathews, D., Disney, M., Childs, J., Schroeder, S., Zuker, M., and Turner, D. (2004). Incorporating chemical modification constraints into a dynamic programming algorithm for prediction of RNA secondary structure. *Proc Natl Acad Sci*, **101**, 7287–7292.
- Mathews, D. H. (2004). Using an RNA secondary structure partition function to determine confidence in base pairs predicted by free energy minimization. *RNA*, **10**(8), 1178–1190.
- McCarthy, B. J. and Holland, J. J. (1965). Denatured DNA as a direct template for in vitro protein synthesis. *Proc. Natl. Acad. Sci. USA*, **54**(3), 880–886.
- McCaskill, J. S. (1990). The equilibrium partition function and base pair binding probabilities for RNA secondary structure. *Biopolymers*, **29**, 1105–1119.
- Miklós, I., Meyer, I., and Nagy, B. (2005). Moments of the boltzmann distribution for RNA secondary structures. *Bull. Math. Biol.*, **67**(5), 1031–47.
- Mount, D. M. (2004). *Bioinformatics: Sequence and Genome Analysis*. Cold Spring Harbor Laboratory Press, 2nd ed. edition.
- Nussinov, R., Piecznik, G., Griggs, J. R., and Kleitman, D. J. (1978). Algorithms for loop matching. *SIAM J. Appl. Math.*, **35**(1), 68–82.
- Orland, H. and Zee, A. (2002). RNA folding and large n matrix theory. *Nuclear Physics B*, **620**, 456–476.
- Parisien, M. and Major, F. (2008). The MC-Fold and MC-Sym pipeline infers RNA structure from sequence data. *Nature*, **452**, 51–55.
- Penner, R. C. (2004). Cell decomposition and compactification of Riemann’s moduli space in decorated Teichmüller theory. In N. Tongring and R. C. Penner, editors, *Woods Hole Mathematics-perspectives in math and physics*, pages 263–301. World Scientific, Singapore. arXiv: math.GT/0306190.
- Penner, R. C. and Waterman, M. S. (1993). Spaces of RNA secondary structures. *Adv. Math.*, **101**, 31–49.
- Reidys, C. M., Huang, F., Andersen, J. E., Penner, R. C., Stadler, P. F., and Nebel, M. E. (2011). Topology and prediction of RNA pseudoknots. *Bioinformatics*, **27**, 1076–1085.
- Rivas, E. and Eddy, S. R. (1999). A dynamic programming algorithm for RNA structure prediction including pseudoknots. *J. Mol. Biol.*, **285**, 2053–2068.
- Rivas, E. and Eddy, S. R. (2000). The language of RNA: A formal grammar that includes pseudoknots. *Bioinformatics*, **16**, 334–340.
- Schuster, P. (1997). Genotypes with phenotypes: adventures in an RNA toy world. *Biophys. Chem.*, **66**(2-3), 75–110.
- Schuster, P., Fontana, W., Stadler, P. F., and Hofacker, I. L. (1994). From sequences to shapes and back: a case study in RNA secondary structures. *Proc Biol Sci.*, **255**(1344), 279–84.
- Shi, H. and Moore, P. B. (2000). The crystal structure of yeast phenylalanine tRNA at 1.93 Å resolution: a classic structure revisited. *RNA*, **6**, 1091–1105.
- Smith, T. and Waterman, M. (1978). RNA secondary structure. *Math. Biol.*, **42**, 31–49.
- Tacker, M., Stadler, P. F., Bornberg-Bauer, E. G., Hofacker, I. L., and Schuster, P. (1996). Algorithm independent properties of RNA structure prediction. *Eur. Biophys. J.*, **25**, 115–130.
- Temin, H. and Mizutani, S. (1970). RNA-dependent DNA polymerase in virions of rous sarcoma virus. *Nature*, **226**(5252), 1211–3.
- The 1000 Genomes Project Consortium (2015). A global reference for human genetic variation. *Nature*, **526**(68-74).
- Turner, D. and Mathews, D. H. (2010). NNDB: the nearest neighbor parameter database for predicting stability of nucleic acid secondary structure. *Nucl. Acids Res.*, **38**(Database), 280–282.
- Uzawa, T., Yamagishi, A., and Oshima, T. (2002). Polypeptide synthesis directed by DNA as a messenger in cell-free polypeptide synthesis by extreme thermophiles, thermus thermophilus HB27 and sulfobolus tokodaii strain 7. *J. Biochem*, **131**(6), 849–53.
- von Neumann, J. and Goldstine, H. H. (1947). Numerical inverting of matrices of high order. *Bull. Amer. Math. Soc.*, **53**(11), 1021–1099.
- Waterman, M. S. (1978). Secondary structure of single-stranded nucleic acids. *Adv. Math. (Suppl. Studies)*, **1**, 167–212.
- Zuker, M. and Stiegler, P. (1981). Optimal computer folding of larger RNA sequences using thermodynamics and auxiliary information. *Nucleic Acids Res.*, **9**, 133–148.